

## Chapter 12

# Robust Performance

*However, by building an amplifier whose gain is deliberately made, say 40 decibels higher than necessary (10000 fold excess on energy basis), and then feeding the output back on the input in such a way as to throw away that excess gain, it has been found that extraordinary improvements in constancy of amplification and freedom from non-linearity.*

Harold S. Black, “Stabilized Feedback Amplifiers”, 1934 [Bla34].

The above quote illustrates that one the key uses of feedback is to provide robustness to uncertainty. It is one of the most useful properties of feedback and is what makes it possible to design feedback systems based on strongly simplified models. This chapter focuses on the analysis of robustness of feedback systems. We consider the stability and performance of systems whose process dynamics are uncertain and derive fundamental limits for robust stability and performance. To do this we develop ways to model uncertainty, both in the form of parameter variations and in the form of neglected dynamics. We also discuss how to design controllers to achieve robust performance. One limitation of the tools we present here is that they are usually restricted to linear systems, although some nonlinear extensions have been developed.

### 12.1 Modeling Uncertainty

One form of uncertainty in dynamical systems is that the parameters describing the system are unknown, which is called *parametric uncertainty*. A typical example is the variation of the mass of a car, which changes with the number of passengers and the weight of the baggage. When linearizing a nonlinear system, the parameters of the linearized model also depend on

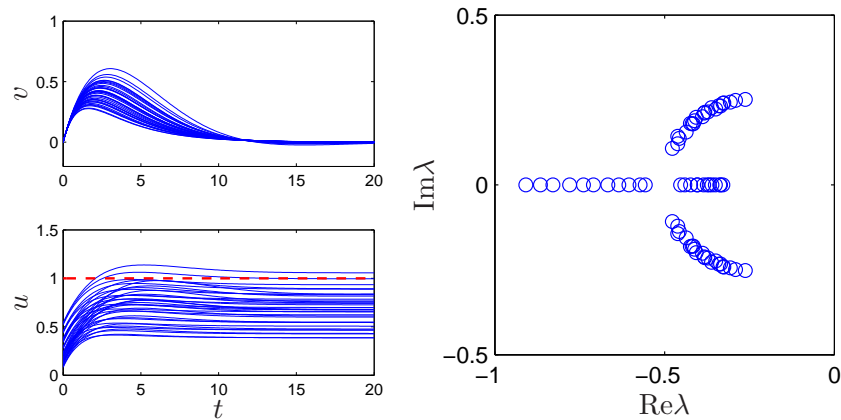


Figure 12.1: Responses of the cruise control system to a slope increase of  $3^\circ$  (left) and the eigenvalues of the closed loop system (right). Model parameters are swept over a wide range.

the operating condition. It is straightforward to investigate effects of parametric uncertainty simply by evaluating the performance criteria for a range of parameters. Such a calculation will directly reveal the consequences of parameter variations. We illustrate by a simple example.

**Example 12.1** (Cruise control). The cruise control problem was described in Section 3.1 and a PI controller was designed in Example 10.1. To investigate the effect of parameter variations we will choose a controller designed for a nominal operating condition corresponding to mass  $m = 1600$ , fourth gear  $\alpha = 12$  and speed  $v = 25$  m/s, the controller gains are  $k = 0.72$  and  $k_i = 0.18$ . Figure 12.1 shows the velocity  $v$  and the throttle  $u$  when encountering a hill with a  $3^\circ$  slope with masses in the range  $1600 < m < 2000$ , gear ratios  $10 \leq \alpha \leq 16$  and velocity  $10 \leq v \leq 40$  m/s. The simulations were done using models that were linearized around the different operating conditions. The figure shows that there are variations in the response but that they are quite reasonable. The largest velocity error is in the range of 0.2 to 0.6 m/s, and the response time is about 15 s. The control signal is marginally larger than 1 in some cases which implies that the throttle is fully open. A full nonlinear simulation using a controller with windup protection is required if we want to explore these cases in more detail. Figure 12.1 also shows the eigenvalues of the closed loop system for the different operating conditions. The figure shows that the closed loop system is well damped in all cases.  $\nabla$

This example indicates that at least as far as parametric variations are concerned, the design based on a simple nominal model will give satisfactory control. The example also indicates that a controller with fixed parameters can be used in all cases. Notice however that we have not considered operating conditions in low gear and at low speed.

## Unmodeled Dynamics

It is generally fairly easy to investigate the effects of parametric variations. There are however other uncertainties that also are important. The simple model of the cruise control system only captures the dynamics of the forward motion of the vehicle and the torque characteristics of the engine and transmission. It does not, for example, include a detailed model of the engine dynamics (whose combustion processes are extremely complex), nor the slight delays that can occur in modern electronically controlled engines (due to the processing time of the embedded computers). These neglected mechanisms that are called *unmodeled dynamics*.

Unmodeled dynamics can be accounted for by developing a more complex model. Such models are commonly used for controller development but it is a substantial effort to develop the models. An alternative is to investigate if the closed loop system is sensitive to generic forms of unmodeled dynamics. The basic idea is to describe the “unmodeled” dynamics by including a transfer function in the system description whose frequency response is bounded, but otherwise unspecified. For example, we might model the engine dynamics in the speed control example as a system that very quickly provides the torque that is requested through the throttle, giving a small deviation from the simplified model, which assumed the torque response was instantaneous. This technique can also be used in many instances to model parameter variations, allowing a quite general approach to uncertainty management.

In particular we wish to explore if additional linear dynamics may cause difficulties. A simple way is to assume that the transfer function of the process is  $P(s) + \Delta P(s)$  where  $P(s)$  is the nominal simplified transfer function and  $\delta_a = \delta P(s)$  represents the unmodeled dynamics. This case is called *additive uncertainty*. Figure 12.2 shows some other cases to represent uncertainties in a linear system.

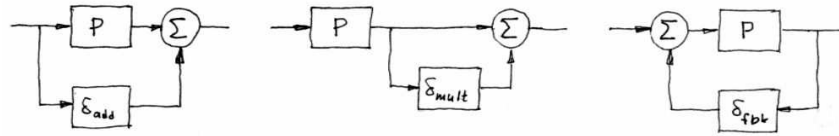


Figure 12.2: Representation of system with additive (left), multiplicative (middle) and feedback uncertainties (right). The nominal system is  $P$  systems and  $\delta$  represents the uncertainties.

### When are Two Systems Similar

A fundamental issue is to determine when two systems are close. This seemingly innocent problem is not as simple as it may appear. A naive idea is to say that two systems are close if their open loop responses are close. Even if this appears natural, there are complications as is illustrated by the following examples.

**Example 12.2** (Similar in open loop but large differences in closed loop). The systems with the transfer functions

$$P_1(s) = \frac{100}{s+1}, \quad P_2(s) = \frac{100}{(s+1)(sT+1)^2}$$

have very similar open loop responses for small values of  $T$ , as illustrated in the top left corner of Figure 12.3, where  $T = 0.025$ . The differences between the step responses are barely noticeable in the figure. The step responses with unit gain error feedback are shown in the figure to the right. Notice that one closed loop system is stable and the other one is unstable. The transfer functions from reference to output are

$$T_1 = \frac{100}{s+101} \quad T_2 = \frac{1161600}{(s+83.93)(s^2-2.92s+1925.37)}.$$

▽

**Example 12.3** (Different in open loop but similar in closed loop). Consider the systems

$$P_1(s) = \frac{100}{s+1}, \quad P_2(s) = \frac{100}{s-1}.$$

The open loop responses have very different because  $P_1$  is stable and  $P_2$  is unstable, as shown in the bottom left plot in Figure 12.3. Closing a feedback

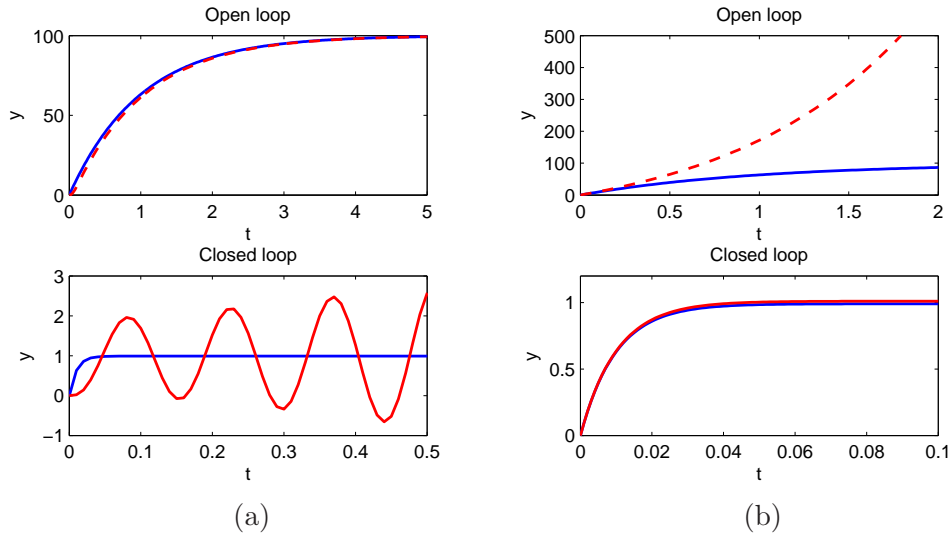


Figure 12.3: Open loop step responses and corresponding closed loop step responses for (a) Example 12.2 and (b) Example 12.3.

loop with unit gain around the systems we find that the closed loop transfer functions are

$$T_1(s) = \frac{100}{s + 101} \quad T_2(s) = \frac{100}{s + 99}$$

which are very close as is also shown in Figure 12.3. ∇

These examples show that if our goal is to close a feedback loop it may be very misleading to compare the open loop responses of the system. Inspired by the examples we will introduce a distance measure that is more appropriate for closed loop operation. Consider two systems with the rational transfer functions

$$P_1(s) = \frac{n_1(s)}{d_1(s)} \quad \text{and} \quad P_2(s) = \frac{n_2(s)}{d_2(s)},$$

where  $n_1(s)$ ,  $n_2(s)$ ,  $d_1(s)$  and  $d_2(s)$  are polynomials. Let

$$p(s) = d_1(s)n_2(-s) - n_1(s)d_2(-s)$$

and define the *chordal distance* between the transfer functions is defined as

$$d_\nu(P_1, P_2) = \begin{cases} \sup_\omega \frac{|P_1(j\omega) - P_2(j\omega)|}{\sqrt{(1+|P_1(j\omega)|^2)(1+|P_2(j\omega)|^2)}} & \text{if } p(s) \text{ has no RHP zeros} \\ 1 & \text{otherwise.} \end{cases} \tag{12.1}$$

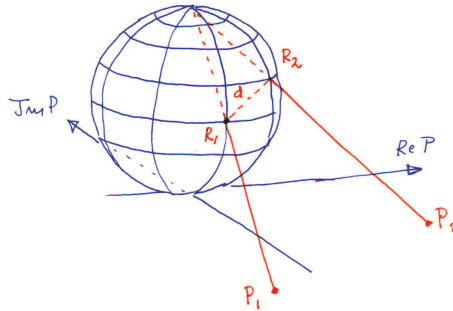


Figure 12.4: Geometric interpretation of the distance  $d(P_1, P_2)$  between two transfer functions.

The distance has a nice geometric interpretation, as shown in Figure 12.4, where the Nyquist plots of  $P_1$  and  $P_2$  are projected on the Riemann sphere. The Riemann sphere is located above the complex plane. It has diameter 1 and its south pole is at the origin of the complex plane. Points in the complex plane are projected onto the sphere by a line through the point and the north pole (Figure 12.4). The distance  $d_\nu(P_1, P_2)$  is simply the shortest chordal distance between the projections of the Nyquist curves. Since the diameter of the Riemann sphere is 1, it follows that the distance is never larger than 1.

The distance  $d_\nu(P_1, P_2)$  is similar to  $|P_1 - P_2|$  when the transfer functions are small, but very different when  $|P_1|$  and  $|P_2|$  are large. It is also related to the behavior of the systems under unit feedback as will be discussed in Section 12.6.

## 12.2 Stability in the Presence of Uncertainty

We begin by considering the problem of robust stability: when can we show that the stability of a system is robust with respect to process variations. This is an important question since the potential for instability is one of the main drawbacks of feedback. Hence we want to ensure that even if we have small inaccuracies in our model, we can still guarantee stability and performance.

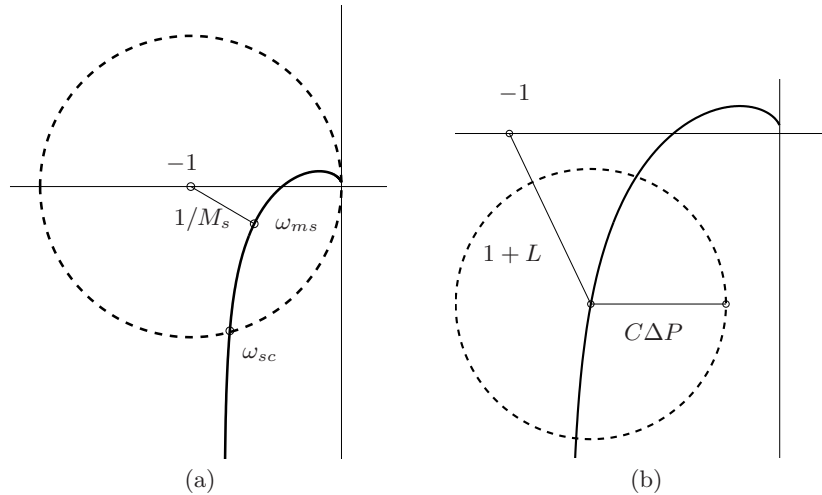


Figure 12.5: The left figure shows that the distance to the critical point  $1/M_s$  is a robustness measure. The right figure shows the Nyquist curve of a nominal loop transfer function and its uncertainty caused by additive process variations  $\Delta P$ .

### Using Nyquist's Stability Criterion

The Nyquist criterion provides a powerful and elegant way to study the effects of uncertainty for linear systems. A simple criterion is that the Nyquist curve is sufficiently far from the critical point  $-1$ . Recall that the shortest distance from the Nyquist curve is  $1/M_s$  where  $M_s$  is the maximum of the sensitivity function. The maximum sensitivity  $M_s$  is thus a good robustness measure, as illustrated Figure 12.5a.

We will now derive explicit conditions for permissible process uncertainties. Consider a feedback system with a process  $P$  and a controller  $C$ . If the process is changed from  $P$  to  $P + \Delta P$ , the loop transfer function changes from  $PC$  to  $PC + C\Delta P$ , as illustrated in Figure 12.5b. If we have a bound on the size of  $\Delta P$  (represented by the dashed circle in the figure), then the system remains stable as long as the process variations never overlap the  $-1$  point, since this leaves the number of encirclements of  $-1$  unchanged.

Some additional assumptions required for the analysis to hold. Most importantly, we require that the process perturbations  $\Delta P$  be stable so that we do not introduce any new right half plane poles that would require additional encirclements in the Nyquist criterion. Also, we note that this condition is conservative: it allows for any perturbation that satisfies the given bounds,

while in practice we may have more information about possible perturbations.

The distance from the critical point  $-1$  to the loop transfer function  $L$  is  $|1 + L|$ . This means that the perturbed Nyquist curve will not reach the critical point  $-1$  provided that

$$|C\Delta P| < |1 + L|,$$

which implies

$$|\Delta P| < \left| \frac{1 + PC}{C} \right| \quad \text{or} \quad \left| \frac{\Delta P}{P} \right| < \frac{1}{|T|}. \quad (12.2)$$

This condition must be valid for all points on the Nyquist curve, i.e. pointwise for all frequencies. The condition for stability can thus be written as

$$\left| \frac{\Delta P(j\omega)}{P(j\omega)} \right| < \frac{1}{|T(j\omega)|} \quad \text{for all } \omega \geq 0. \quad (12.3)$$

This condition allows us to reason about uncertainty without exact knowledge of the process perturbations. Namely, we can verify stability for *any* uncertainty  $\Delta P$  that satisfies the given bound. From an analysis perspective, this gives us a measure of the robustness of a given design. Conversely, if we require robustness of a given level, we can attempt to choose our controller  $C$  such that the desired level of robustness is available (by asking  $T$  to be small).

The formula given by equation (12.3) is one of the reasons why feedback systems work so well in practice. The mathematical models used to design control system are often strongly simplified. There may be model errors and the properties of a process may change during operation. Equation (12.3) implies that the closed loop system will at least be stable for substantial variations in the process dynamics.

It follows from equation (12.3) that the variations can be large for those frequencies where  $T$  is small and that smaller variations are allowed for frequencies where  $T$  is large. A conservative estimate of permissible process variations that will not cause instability is given by

$$\left| \frac{\Delta P(j\omega)}{P(j\omega)} \right| < \frac{1}{M_t},$$

where  $M_t$  is the largest value of the complementary sensitivity

$$M_t = \sup_{\omega} |T(j\omega)| = \left\| \frac{PC}{1 + PC} \right\|_{\infty}. \quad (12.4)$$



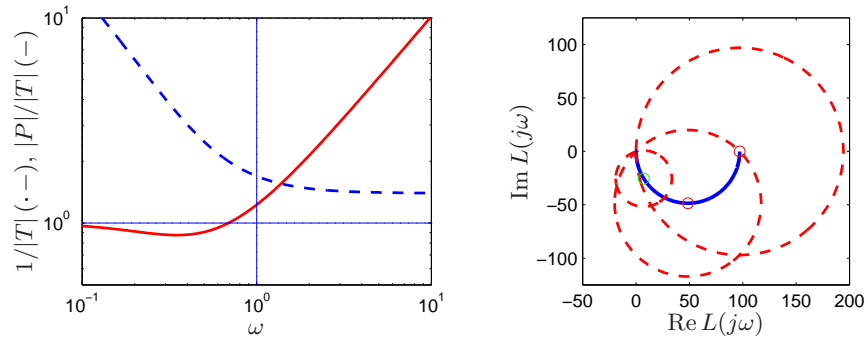


Figure 12.6: Illustration of the robustness for a cruise controller. The left figure shows the maximum relative error ( $1/|T|$ , dot-dashed) and absolute error ( $|P|/|T|$ , solid) for the process uncertainty  $\Delta P$ . The Nyquist curve is shown in the right figure, as a solid line. The dashed circles show permissible perturbations in the process dynamics,  $|\Delta P| = |P|/|T|$ , at the frequencies  $\omega = 0, 0.0142$  and  $0.05$ .

The value of  $M_t$  is influenced by the design of the controller. For example, if  $M_t = 2$  then pure gain variations of 50% or pure phase variations of  $30^\circ$  are permitted without making the closed loop system unstable.

**Example 12.4** (Cruise control). Consider the cruise control system discussed in Section 3.1. The model of the car in fourth gear at speed 25 m/s is

$$P(s) = \frac{1.38}{s + 0.0142},$$

and the controller is a PI controller with gains  $k = 0.72$  and  $k_i = 0.18$ . Figure 12.6 plots the allowable size of the process uncertainty using the bound in equation (12.3). At low frequencies,  $T(0) = 1$  and so the perturbations can be as large as the original process ( $|\Delta P/P| < 1$ ). The complementary sensitivity has its maximum  $M_t = 1.14$  at  $\omega_{mt} = 0.35$  and hence this gives the minimum allowable process uncertainty, with  $|\Delta P/P| < 0.87$  or  $|\Delta P| < 3.47$ . Finally, at high frequencies  $T \rightarrow 0$  and hence the relative error can get very large. For example, at  $\omega = 5$  we have  $|T(j\omega)| = 0.195$  which means that the stability requirement is  $|\Delta P/P| < 5.1$ . The analysis clearly indicates that the system has good robustness and that the high frequency properties of the transmission system are not important for the design of the cruise controller.

Another illustration of the robustness of the system is given in the right diagram of Figure 12.6, which shows the Nyquist curve of the transfer func-

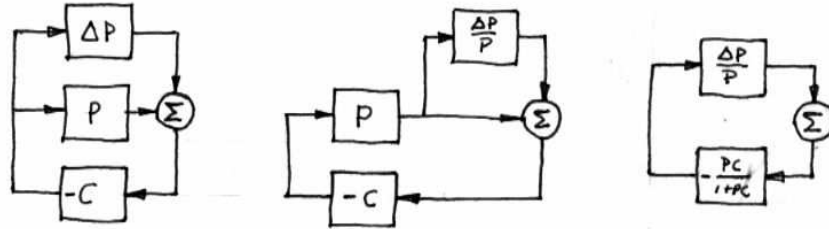


Figure 12.7: Illustration of robustness to process perturbations.

tion of the process and the uncertainty bounds  $\Delta P = |P|/|T|$  for a few frequencies. Note that the controller can tolerate very large amounts of uncertainty and still maintain stability of the closed loop.  $\nabla$

The situation illustrated in the previous example is typical for many processes: moderately small uncertainties are only required around the gain crossover frequencies, but large uncertainties can be permitted at higher and lower frequencies. A consequence of this is that a simple model that describes the process dynamics well around the crossover frequency is often sufficient for design. Systems with many resonance peaks are an exception to this rule because the process transfer function for such systems may have large gains also for higher frequencies.

Notice that the results we have given can be very conservative. Referring to Figure 12.5, the critical perturbations, which were the basis for our analysis, are in the direction towards the critical point. It is possible to have much larger perturbations in the opposite direction.



### The Small Gain Theorem

The robustness result given by equation (12.3) can be given another interpretation by using the small gain theorem, introduced in Section 9.5. It is convenient to choose a particular form of the small gain theorem where the gain of a system is defined in terms of the maximum amplitude of the frequency response. We first define the gain of a system as the  $H_\infty$  norm of its transfer function  $H(s)$ :

$$\|H\|_\infty = \sup_{\omega} |H(j\omega)|.$$

The small gain theorem can now be written as follows.

Table 12.1: Conditions for robust stability for different types of uncertainty

| Process                    | Type           | Robust Stability            |
|----------------------------|----------------|-----------------------------|
| $P + \Delta P$             | Additive       | $\ CS\Delta P\ _\infty < 1$ |
| $P(1 + \Delta P)$          | Multiplicative | $\ S\Delta P\ _\infty < 1$  |
| $P/(1 + \Delta P \cdot P)$ | Feedback       | $\ PS\Delta P\ _\infty < 1$ |

**Theorem 12.1** (Small gain theorem). *Consider two stable, linear time invariant processes with transfer functions  $P_1(s)$  and  $P_2(s)$ . The feedback interconnection of these two systems is stable if  $\|P_1P_2\|_\infty < 1$ .*

The proof of this theorem follows directly from the Nyquist criterion applied to the loop transfer functions  $L = P_1P_2$ .

The application of this theorem is illustrated in Figure 12.7, which shows a sequence of block diagrams of a closed loop system with a perturbed process. Using block diagram manipulation, we can isolate the uncertainty from the remaining dynamics and obtain the two block interconnection shown in Figure 12.7c. The loop transfer function of the resulting system is

$$L = \frac{PC}{1 + PC} \frac{\Delta P}{P} = T\Delta P = CS\Delta P.$$

Equation (12.3) implies that the largest loop gain is less than one and hence the systems is stable via the small gain theorem.

The small gain theorem can be used to check robust stability for uncertainty in a variety of situations. Table 12.1 summarizes a few of the common cases; the proofs (all via the small gain theorem) are left to the exercises.

## Youla Parameterization



Since stability is such an essential property it is useful to characterize all controller that will stabilize a given process. Consider a stable process with the rational transfer function  $P$ , to simplify the writing we drop the arguments of the functions. A system with the complementary sensitivity function  $T$  can be obtained by feedforward control with the stable transfer function  $Q$  if

$$T = PQ \tag{12.5}$$

Notice that  $T$  must have the same RHP zeros as  $P$  since  $Q$  is stable. Now assume that we want to obtain the complementary transfer function  $T$  by

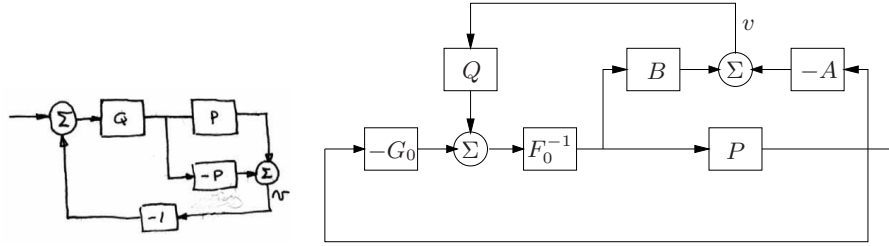


Figure 12.8: Block diagrams of Youla parameterizations of stable (left) and unstable systems (right). Notice that the signal  $v$  is zero.

using unit feedback with the controller  $C$ . Since  $T = PC/(1 + PC) = PQ$  we find that the controller transfer function is

$$C = \frac{Q}{1 - QP}. \quad (12.6)$$

A straight forward calculation gives

$$\frac{1}{1 + PC} = 1 - T, \quad \frac{P}{1 + PC} = P - PT, \quad \frac{C}{1 + PC} = Q, \quad \frac{PC}{1 + PC} = T$$

which are all stable. All stabilizing controller are thus given by equation (12.6). Equation (12.6) is called a *Youla parameterization* because it characterizes all controllers that stabilizes a stable process. The parameterization is be illustrated by the block diagrams in Figure 12.8.

The feedforward controller (12.5) is given by  $Q = P^{-1}T$ . In particular if it is desired to have  $T$  close to one it follows that the feedforward controller is the inverse of the process transfer function. Comparing with the feedback controller (12.6) we find that the feedback controller obtains the desired result by using high gain feedback.

A similar characterization can be obtained also for unstable systems. Consider a process with a rational transfer function  $P = a/b$  where  $a$  and  $b$  are polynomials, by introducing a stable polynomial  $c$  we can write

$$P(s) = \frac{a}{b} = \frac{A}{B},$$

where  $A = a/c$  and  $B = b/c$  are stable rational functions. We have

$$\begin{aligned} \frac{1}{1 + PC_0} &= \frac{AF_0}{AF_0 + BG_0} = S_0 & \frac{P}{1 + PC_0} &= \frac{BF_0}{AF_0 + BG_0} = PS_0 \\ \frac{C_0}{1 + PC_0} &= \frac{AG_0}{AF_0 + BG_0} = CS_0 & \frac{PC_0}{1 + PC_0} &= \frac{BG_0}{AF_0 + BG_0} = T_0 \end{aligned}$$

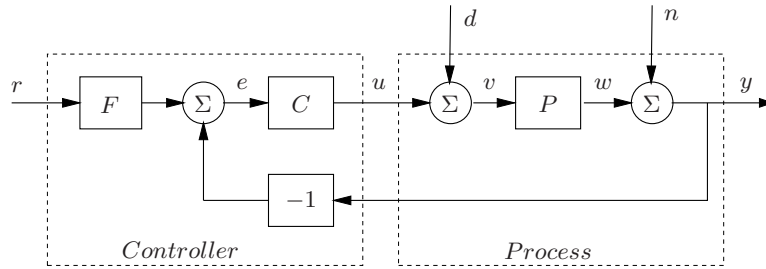


Figure 12.9: Block diagram of a basic feedback loop.

Since  $C$  is a stabilizing controller the function  $AF_0 + BG_0$  must have all its zeros in the left half plane. All stabilizing controllers are now given by

$$C = \frac{G_0 + QA}{F_0 - QB}. \quad (12.7)$$

We have

$$\begin{aligned} \frac{1}{1 + PC} &= \frac{A(F_0 - QG)}{AF_0 + BG_0} & \frac{P}{1 + PC} &= \frac{BF_0 - QB^2}{AF_0 + BG_0} \\ \frac{C}{1 + PC} &= \frac{AG_0 + QA^2}{AF_0 + BG_0} & \frac{PC}{1 + PC} &= \frac{AF_0 + BG_0}{AF_0 + BG_0}. \end{aligned}$$

All these transfer functions are stable and equation(12.7) is therefore a Youla parameterization. Notice that equation (12.7) reduces to equation(12.6) for  $F_0 = 1$  and  $G_0 = 0$ .

## 12.3 Performance in the Presence of Uncertainty

So far we have investigated the risk for instability and robustness to process uncertainty. We will now explore how responses to load disturbances, measurement noise and command signal following are influenced by process variations. To do this we will analyze the system in Figure 12.9.

### Disturbance Attenuation

A simple criterion for disturbance attenuation is to compare the output of the closed loop system in Figure 12.9 with the output of the corresponding open loop system. If we let the disturbances for the open and closed loop systems be identical, the output of the closed loop system is then obtained

simply by passing the open loop output through a system with the transfer function  $S$ . The sensitivity function thus tells how the variations in the output are influenced by feedback. Disturbances with frequencies such that  $|S(j\omega)| < 1$  are attenuated but disturbances with frequencies such that  $|S(j\omega)| > 1$  are amplified by feedback. The maximum sensitivity  $M_s$  and the sensitivity crossover frequency  $\omega_{sc}$  are simple performance measures.

The sensitivity function  $S$  gives a gross characterization of the effect of feedback on disturbances. A more detailed characterization is given by the transfer function from load disturbances to process output:

$$G_{yd} = \frac{P}{1 + PC} = PS. \quad (12.8)$$

Load disturbances typically have low frequencies and it is therefore important that the transfer function is small for low frequencies. For processes with constant low frequency gain and a controller with integral action we have  $G_{yd} \approx s/k_i$ . Integral gain  $k_i$  is thus a simple measure of attenuation of load disturbances.

To find how the transfer function  $G_{yd}$  is influenced by small variations in the process transfer function we differentiate equation (12.8) which gives

$$\frac{dG_{yd}}{G_{yd}} = S \frac{dP}{P}. \quad (12.9)$$

The response to load disturbances is thus insensitive to process variations for frequencies where  $|S(j\omega)|$  is small, i.e. for those frequencies where load disturbances are important.

A drawback with feedback is that the controller feeds measurement noise into the system. In addition to the load disturbance rejection, it thus is also important that the control actions generated by measurement noise are not too large. It follows from Figure 12.9 that the transfer function  $G_{un}$  from measurement noise to controller output is given by

$$G_{un} = -\frac{C}{1 + PC} = -\frac{T}{P} \quad (12.10)$$

Since measurement noise typically has high frequencies it is important that the transfer function  $G_{un}$  is not too large for high frequencies. The loop transfer function  $PC$  is typically small for high frequencies, which implies that  $G_{un} \approx C$  for large  $s$ . To avoid injecting too much measurement noise it is therefore important that  $C(s)$  is small for large  $s$ . This property is called high frequency roll-off. Filtering of the measured signal in a PID controller is done to reduce injection of measurement noise, see Section 10.5.

To find how the transfer function  $G_{un}$  is influenced by small variations in the process transfer function we differentiate equation (12.10) which gives

$$\frac{dG_{un}}{G_{un}} = T \frac{dP}{P}. \quad (12.11)$$

Measurement noise typically has high frequencies. Since the complementary sensitivity function also is small for high frequencies we find that process uncertainty has little influence on the transfer function  $G_{un}$  for frequencies where measurement are important.

### Command Signal Following

The transfer function from reference to output is given by

$$G_{yr} = \frac{PCF}{1 + PC} = T, \quad (12.12)$$

which is the complementary sensitivity function. To see how variations in  $P$  affect the performance of the system, we differentiate equation (12.12) with respect to the process transfer function:

$$\frac{dG_{yr}}{dP} = \frac{CF}{1 + PC} - \frac{PCFC}{(1 + PC)^2} = \frac{CF}{(1 + PC)^2} = S \frac{G_{yr}}{P}.$$

and it follows that

$$\frac{dG_{yr}}{G_{yr}} = S \frac{dP}{P}. \quad (12.13)$$

The relative error in the closed loop transfer function thus equals the product of the sensitivity function and the relative error in the process. In particular, it follows from equation (12.13) that the relative error in the closed loop transfer function is small when the sensitivity is small. This is one of the very useful properties of feedback.

When analyzing robust stability we were able to deal with large disturbances. In this section we have limited the analysis to small (differential) perturbations. There are some additional assumptions required for the analysis to hold. Most importantly, we require that the process perturbations  $dP$  be stable so that we do not introduce any new right half plane poles that would require additional encirclements in the Nyquist criterion. Also, we note that this condition is conservative: it allows for any perturbation that satisfies the given bounds, while in practice we have more information about possible perturbations.

## 12.4 Limits on the Sensitivities

The sensitivity function  $S$  and the complementary sensitivity function  $T$  tell us a great deal about the feedback loop. Disturbance rejection and sensitivity to process uncertainties are low for frequencies where  $S$  is small and tracking performance is good when  $T$  is close to 1. In this section we explore some of the limitations on robust performance by looking at algebraic and integral constraints on the functions.

Since

$$S = \frac{1}{1 + PC} \quad \text{and} \quad T = \frac{PC}{1 + PC}$$

it follows that the sensitivity functions are related through

$$S + T = 1. \tag{12.14}$$

A useful design goal is to make  $S$  close to zero and  $T$  close to one, a design goal that is compatible with equation (12.14). The loop transfer function  $L$  is typically large for small values of  $s$  and it goes to zero as  $s$  goes to infinity. This means that  $S$  is typically small for small  $s$  and close to 1 for large  $s$ . The complementary sensitivity function is close to 1 for small  $s$  and it goes to 0 as  $s$  goes to infinity.

### Bode's Integral Formula

A basic problem is to investigate if  $S$  can be made small over a large frequency range. We will start by investigating an example.

**Example 12.5** (System that admits small sensitivities). Consider a closed loop system consisting of a first order process and a proportional controller. Let the loop transfer function

$$L = PC = \frac{k}{s + 1}$$

where parameter  $k$  is the controller gain. The sensitivity function is

$$S = \frac{s + 1}{s + 1 + k}$$

and we have

$$|S(j\omega)| = \sqrt{\frac{1 + \omega^2}{1 + 2k + k^2 + \omega^2}}$$

This implies that  $|S(j\omega)| < 1$  for all finite frequencies and that the sensitivity can be made arbitrary small for any finite frequency by making  $k$  sufficiently large. ∇



The system in Example 12.5 is unfortunately an exception. The key feature of the system is that the Nyquist curve of the process is completely contained in the right half plane. Such systems are called *positive real*. For these systems the Nyquist curve never enters the region shown in Figure 11.6 where the sensitivity is greater than one.

For typical control systems there are unfortunately severe constraints on the sensitivity function. The following theorem, due to Bode, provides fundamental insights into the limits of performance under feedback.

**Theorem 12.2** (Bode's integral formula). *Let  $S(s)$  be the sensitivity function for a feedback system and assume that it goes to zero faster than  $1/s$  for large  $s$ . If the loop transfer has poles  $p_k$  in the right half plane then the sensitivity function satisfies the following integral:*

$$\int_0^\infty \log |S(j\omega)| d\omega = \int_0^\infty \log \frac{1}{|1 + L(j\omega)|} d\omega = \pi \sum \operatorname{Re} p_k. \quad (12.15)$$

Equation (12.15) implies that there are fundamental limitations to what can be achieved by control and that control design can be viewed as a redistribution of disturbance attenuation over different frequencies. This equation shows that if the sensitivity function is made smaller for some frequencies it must increase at other frequencies. This means that if disturbance attenuation is improved in one frequency range it will be worse in other. This is called the *waterbed effect*. It also follows that systems with poles in the right half plane have larger sensitivity.

For a loop transfer function without poles in the right half plane equation (12.15) reduces to

$$\int_0^\infty \log |S(j\omega)| d\omega = 0.$$

This formula can be given a nice geometric interpretation as shown in Figure 12.10, which shows  $\log |S(j\omega)|$  as a function of  $\omega$ . The area over the horizontal axis must be equal to the area under the axis when frequency is plotted on a *linear* scale.

There is an analogous result for the complementary sensitivity function which tells that

$$\int_0^\infty \log |T(\frac{1}{j\omega})| d\omega = \pi \sum \frac{1}{z_i},$$

where the summation is over all right half plane zeros. Notice that small right half plane zeros are worse than large ones and that large right half plane poles are worse than small ones.

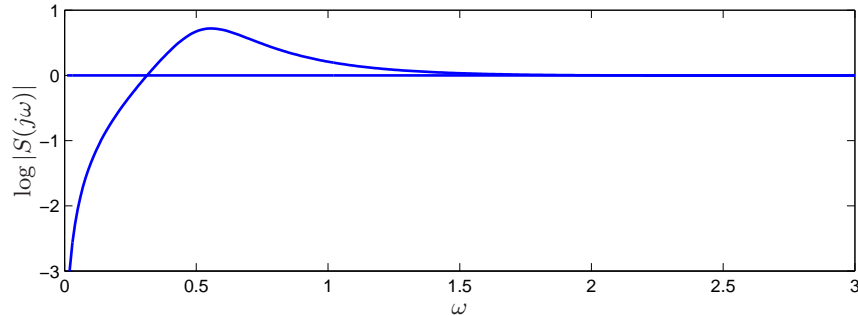


Figure 12.10: Geometric interpretation of the *waterbed effect* given by Bode's integral formula (12.15).



### Derivation of Bode's Formula

This is a technical section which requires some knowledge of the theory of complex variables, in particular contour integration. Assume that the loop transfer function has distinct poles at  $s = p_k$  in the right half plane and that  $L(s)$  goes to zero faster than  $1/s$  for large values of  $s$ .

Consider the integral of the logarithm of the sensitivity function  $S(s) = 1/(1 + L(s))$  over the contour shown in Figure 12.11.

The contour encloses the right half plane except the points  $s = p_k$  where the loop transfer function  $L(s) = P(s)C(s)$  has poles and the sensitivity function  $S(s)$  has zeros. The direction of the contour is counter clockwise.

The integral of the log of the sensitivity function around this contour is given by

$$\begin{aligned} \int_{\Gamma} \log(S(s)) ds &= \int_{jR}^{-jR} \log(S(s)) ds + \int_R \log(S(s)) ds + \sum_k \int_{\gamma_k} \log(S(s)) ds \\ &= I_1 + I_2 + I_3 = 0, \end{aligned}$$

where  $R$  is a large semi circle on the right and  $\gamma_k$  is the contour starting on the imaginary axis at  $s = \text{Im} p_k$  and a small circle enclosing the pole  $p_k$ . The integral is zero because the function  $\log S(s)$  is regular inside the contour. We have

$$I_1 = -j \int_{-jR}^{jR} \log(S(j\omega)) d\omega = -2j \int_0^{jR} \log(|S(j\omega)|) d\omega$$

because the real part of  $\log S(j\omega)$  is an even function and the imaginary

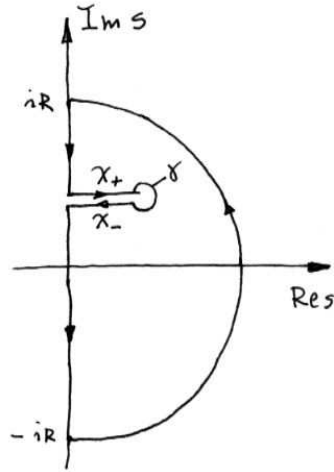


Figure 12.11: Contour used to prove Bode’s theorem. To avoid clutter we have shown only one of the paths that enclose the right half plane.

part is an odd function. Furthermore we have

$$I_2 = \int_R \log(S(s)) ds = \int_R \log(1 + L(s)) ds \approx \int_R L(s) ds.$$

Since  $L(s)$  goes to zero faster than  $1/s$  for large  $s$  the integral goes to zero when the radius of the circle goes to infinity.

Next we consider the integral  $I_3$ , for this purpose we split the contour into three parts  $X_+$ ,  $\gamma$  and  $X_-$  as indicated in Figure 12.11. We can then write the integral as

$$I_3 = \int_{X_+} \log S(s) ds + \int_{\gamma} \log S(s) ds + \int_{X_-} \log S(s) ds.$$

The contour  $\gamma$  is a small circle with radius  $r$  around the pole  $p_k$ . The magnitude of the integrand is of the order  $\log r$  and the length of the path is  $2\pi r$ . The integral thus goes to zero as the radius  $r$  goes to zero. Furthermore, making use of the fact that  $X_-$  is oriented oppositely from  $X_+$ , we have

$$\int_{X_+} \log S(s) ds + \int_{X_-} \log S(s) ds = \int_{X_+} (\log S(s) - \log S(s - 2\pi j)) ds = 2\pi p_k.$$

Since  $|S(s)| = |S(s - 2\pi j)|$  we have

$$\log S(s) - \log S(s - 2\pi j) = \arg S(s) - \arg S(s - 2\pi j) = 2\pi$$

and we find that

$$I_3 = 2\pi \sum p_k$$

Letting the small circles go to zero and the large circle go to infinity and adding the contributions from all right half plane poles  $p_k$  gives

$$I_1 + I_2 + I_3 = -2i \int_0^R \log |S(j\omega)| d\omega + \sum_k 2\pi p_k = 0.$$

which is Bode's formula (12.15).

## 12.5 Robust Pole Placement

Many design methods for control systems do not take robustness into account. In such cases it is essential to always investigate the robustness because there are seemingly reasonable designs that give controller with poor robustness. Any design method which does not take robustness explicitly into account can give controllers with poor robustness. We illustrate this by analyzing controllers designed by state feedback and observers. The closed loop poles can be assigned to arbitrary locations if the system is observable and controllable. However if we want to have a robust closed loop system, the poles and zeros of the process impose severe restrictions on the location of the closed loop poles. Some examples are first given; based on analysis of these examples we then obtain design rules for robust pole placement.

### Slow Stable Zeros

We will first explore the effects of slow stable zeros, and we begin with a simple example.

**Example 12.6** (Vehicle steering). Consider the linearized model for vehicle steering in Example 8.4 which has the transfer function.

$$P(s) = \frac{0.5s + 1}{s^2}.$$

A controller based on an observer and state feedback, where the closed loop poles were given by  $\omega_c = 1$ ,  $\zeta_c = 0.707$ ,  $\omega_o = 2$  and  $\zeta_o = 0.707$  was designed in Example 7.3. Assume that we want a faster closed loop system and choose  $\omega_c = 10$ ,  $\zeta_c = 0.707$ ,  $\omega_o = 20$  and  $\zeta_o = 2$ . A pole assignment design

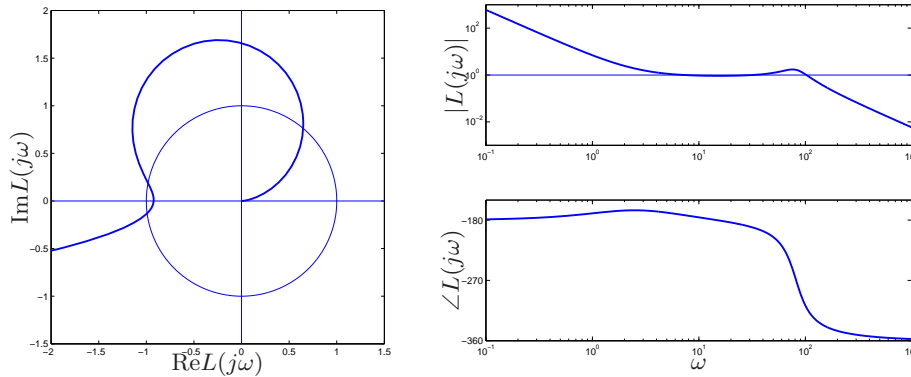


Figure 12.12: Nyquist (left) and Bode (right) plots of the loop transfer function for vehicle steering with a controller based on state feedback and an observer.

gives state feedback gain  $k_1 = 100$  and  $k_2 = -35.86$  and an observer gains  $l_1 = 28.28$  and  $l_2 = 400$ . The controller transfer function is

$$C(s) = \frac{-11516s + 40000}{s^2 + 42.4s + 6657.9}.$$

Figure 12.12 shows Nyquist and Bode plots of the loop transfer function. The Nyquist plot indicates that the robustness is very poor since the loop transfer function is very close to the critical point  $-1$ . The phase margin is only  $7^\circ$ . This also shows up in the Bode plot where the gain curve hovers around the value 1 and the phase curve is close to  $180^\circ$  for a wide frequency range.

More insight is obtained by analyzing the sensitivity functions. The full lines in Figure 12.13 shows the sensitivity functions. The maximum sensitivities are  $M_s = 13$  and  $M_t = 12$ , which are much too large indicating that the system has very poor robustness.  $\nabla$

At first sight it is very surprising that a controller where the nominal system has well damped poles and zeros which are far to the left in the right half plane is so sensitive to process variations. We have an indication that something is unusual because the controller has a zero  $s = 3.9$  in the right half plane. To understand what happens we will investigate the reason for the peaks of the sensitivity functions. Let the transfer functions of the process and the controller be

$$P(s) = \frac{n_p(s)}{d_p(s)} \quad C(s) = \frac{n_c(s)}{d_c(s)},$$

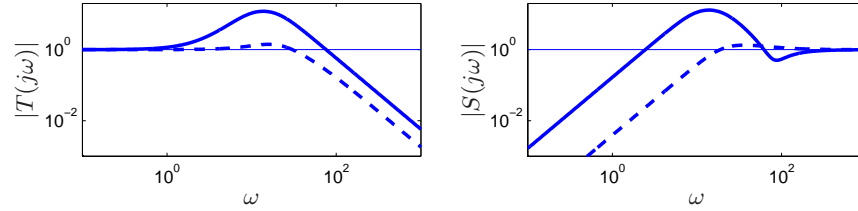


Figure 12.13: Sensitivity function for the system with  $\omega_c = 10$ ,  $\zeta_c = 0.707$ ,  $\omega_o = 20$ ,  $\zeta_o = 0.707$  (solid) and with  $\omega_c = 10$ ,  $\zeta_c = 2.6$  (dashed).

where  $n_p(s)$ ,  $n_c(s)$ ,  $d_p(s)$  and  $d_c(s)$  are polynomials.

The complementary sensitivity function is

$$T(s) = \frac{PC}{1 + PC} = \frac{n_p(s)n_c(s)}{d_p(s)d_c(s) + n_p(s)d_p(s)}.$$

It is 1 for low frequency and start to increase at its first zero which is the process zero at  $s = 2$ , it increases further at the controller zero at  $s = 3.9$  and it does not start to decrease until the closed loop poles appear at  $\omega_c = 10$  and  $\omega_o = 20$ . We can thus conclude that there will be a peak in the complementary sensitivity function. The magnitude of the peak depends on the ratio of the zeros and the poles of the transfer function.

The peak of the complementary sensitivity function can be avoided by assigning a closed loop zero close to the slow process zero. We can achieve this by choosing  $\omega_c = 10$  and  $\zeta_c = 2.6$  which gives the closed loop poles at  $s = -2$  and  $s = -50$ . The controller transfer function then becomes

$$C(s) = \frac{3628s + 40000}{s^2 + 80.28s + 156.56} = 3628 \frac{s + 11.02}{(s + 2)(s + 78.28)}$$

The sensitivity functions are shown in dashed lines in Figure 12.13. The controller gives the maximum sensitivities  $M_s =$  and  $M_t =$  which give a good robustness. Notice that the controller has a pole at  $s = 2$  which cancels the slow process zero. The design can also be done simply by canceling the slow stable process zero and designing the system for the simplified system. One lesson from the example is that it is necessary to choose closed loop poles that are equal to or close to slow stable process zeros. Another lesson is that slow unstable process zeros impose limitations on the achievable bandwidth as was already noted in Section 11.4.

### Fast Stable Process Poles

The next example shows the effect of fast stable poles.

**Example 12.7** (Fast system poles). Consider PI control of a first order system, where the process and the controller have the transfer functions

$$P(s) = \frac{b}{s+a} \quad C(s) = k + \frac{k_i}{s}.$$

The loop transfer function is

$$L(s) = \frac{b(ks + k_i)}{s(s+a)}$$

The closed loop characteristic polynomial is

$$s(s+a) + b(ks + k_i) = s^2 + (a+bk)s + k_i$$

Let the desired closed loop characteristic polynomial be

$$(s+p_1)(s+p_2),$$

we find that the controller parameters are given by

$$k = \frac{p_1 + p_2 - a}{b} \quad k_i = \frac{p_1 p_2}{b}.$$

The sensitivity functions are then

$$S(s) = \frac{s(s+a)}{(s+p_1)(s+p_2)} \quad T(s) = \frac{(p_1 + p_2 - a)s + p_1 p_2}{(s+p_1)(s+p_2)}.$$

Assume that the process pole  $a$  is much larger than the closed loop poles  $p_1$  and  $p_2$ , say  $a > p_2 > p_1$ . Notice that the proportional gain is negative and that the controller has a zero in the left half plane if  $a > p_1 + p_2$ , an indication that the system has bad properties..

Next consider the sensitivity function, which is 1 for high frequencies. Moving from high to low frequencies we find that the sensitivity increases at the process pole  $s = a$ . The sensitivity does not decrease until the closed loop poles are reached resulting in a large sensitivity peak which is approximately  $a/p_2$ . The magnitude of the sensitivity function is shown in Figure 12.14 for  $a = b = 1$ ,  $p_1 = 0.05$ ,  $p_2 = 0.2$ . Notice the high sensitivity peak. For comparison we have also shown the gain curve for the when the process pole is slower than the process pole ( $a = b = a$ ,  $p_1 = 5$ ,  $p_2 = 200$ ). The problem

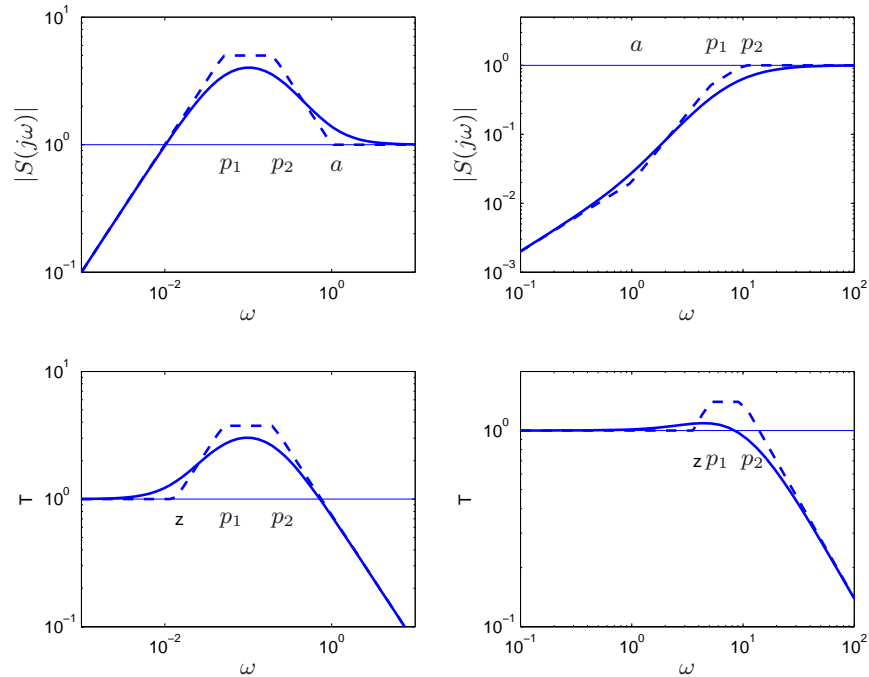


Figure 12.14: Gain curves for Bode plots of the sensitivity function  $S$  for designs with  $p_1 < p_2 < a$  (left) and  $a < p_1 < p_2$  (right). The full lines are the true sensitivities and the dashed lines are the asymptotes

with the poor robustness can be avoided by choosing one closed loop pole equal to the process pole, i.e.  $p_2 = a$ . The controller gains then becomes

$$k = \frac{p_1}{b} \quad k_i = \frac{ap_1}{l},$$

which means that the fast process pole is canceled by a controller zero. The loop transfer function and the sensitivity functions are

$$L(s) = \frac{bk}{s} \quad S(s) = \frac{s}{s + bk} \quad T(s) = \frac{bk}{s + bk}.$$

The maximum sensitivities are less than 1 for all frequencies.  $\nabla$

### Design Rules for Pole-Placement

Based on the insight gained from the examples it is now possible to obtain design rules that give designs with good robustness. Consider the expres-



sion (12.5) for the complementary sensitivity function. Let  $w_{gc}$  be the desired gain crossover frequency. Assume that the process has zeros which are slower than  $\omega_{gc}$ . The complementary sensitivity function is one for low frequencies and it increases for frequencies close to the process zeros unless there is a closed loop pole in the neighborhood. To avoid large values of the complementary sensitivity function we find that the closed loop system should have poles close to or equal to the slow stable zeros. This means that slow stable zeros should be canceled by controller poles. Since unstable zeros cannot be canceled slow stable zeros the presence of slow unstable zeros means that achievable gain crossover frequency must be smaller than the slowest unstable process zero, (see Section 11.3).

Now consider process poles that are faster than the desired gain crossover frequency. Consider the expression (12.5) for the sensitivity function. The sensitivity function is 1 for high frequencies. Moving from high to low frequencies the sensitivity function increases at the fast process poles. Large peaks can be obtained unless there are closed loop poles close to the fast process poles. To avoid large peaks in the sensitivity the closed loop system should be have poles close that matches the fast process poles. This means that the controller should cancel the fast process poles by controller zeros. Since unstable modes cannot be canceled, the presence of a fast unstable pole implies that the gain crossover frequency must be sufficiently large, (see Section 11.3).

To summarize, we obtain the following simple design rule: slow stable process zeros should be matched slow closed loop poles and fast stable process poles should be matched by fast process poles. Slow unstable process zeros and fast unstable process poles impose severe limitations.

## 12.6 Design for Robust Performance

Control design is a rich problem where many factors have to be taken into account. Typical requirements are that load disturbances should be attenuated, the controller should only inject a moderate amount of measurement noise, the output should follow variations in the command signal well and the closed loop system should be insensitive to process variations. For the system in Figure 12.9 these requirements can be captured by specifications on the sensitivity functions  $S$  and  $T$  and the transfer functions  $G_{yd}$ ,  $G_{un}$ ,  $G_{yr}$  and  $G_{ur}$ . Notice that it is necessary to consider at least six transfer functions, as discussed Section 11.1. The requirements are mutually conflicting and it is necessary to make trade-offs. Attenuation of load disturbances will

be improved if the bandwidth is increased but so will the noise injection.

It is highly desirable to have design methods that can guarantee robust performance. Such design methods did not appear until the late 1980. There are many issues to consider in control design. It is interesting that many design methods result in controllers having the same structure as the controller based on state feedback and an observer.

### Linear Quadratic Control LQG

One way to make the trade-off between attenuation of load disturbances and injection of measurement noise is to design a controller which minimizes the loss function

$$J = \frac{1}{T} \int_0^T (y^2(t) + \rho u^2(t)) dt,$$

where  $\rho$  is a weighting parameters as discussed in Section 6.5. This loss function gives a compromise between load disturbance attenuation and disturbance injection because it balances control actions against deviations in the output. If all state variables are measured, the controller is a state feedback

$$u = K(x_m - x).$$

The controller has the same form as the controller obtained by pole assignment in Section 6.2. The controller gain is, however, obtained by solving the optimization problem. It has been shown that this controller is very robust. It has a phase margin of at least  $60^\circ$  and an infinite gain margin. The controller is called a *linear quadratic control* or *LQ control* because the process model is linear and the criterion is quadratic.

When all state variables are not measured, the state can be reconstructed using an observer as discussed in Section 7.3. It is also possible to introduce process disturbances and measurement noise explicitly in the model and to reconstruct the states using a Kalman filter. The Kalman filter has the same structure as the observer designed by pole assignment in Section 7.3, but the observer gains  $L$  are now obtained by solving an optimization problem. The control law obtained by combining linear quadratic control with a Kalman filter is called *linear quadratic Gaussian control* or *LQG Control*. The Kalman filter is optimal when the models for load disturbances and measurement noise are Gaussian.

It is interesting that the solution to the optimization problem leads to a controller having the structure of a state feedback and an observer. The state-feedback gains depend on the parameter  $\rho$  and the filter gains depend

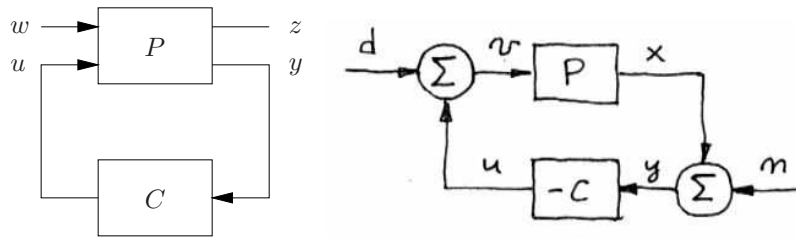


Figure 12.15: The left figure shows a general representation of a control problem used in robust control. The input  $u$  represents the control signal, the input  $w$  represents the external influences on the system, the output  $z$  is the generalized error and the output  $y$  is the measured signal. The right figure shows the special case of the system in Figure 12.9 where the reference signal is zero. In this case we have  $w = (-n, d)$  and  $z = (x, v)$ .

on the parameters in the model that characterize process noise and measurement noise, see Section 7.4. There are efficient programs to compute the feedback and observer gains.

The nice robustness properties of state feedback are unfortunately lost when the observer is added. It is possible to choose parameters which give closed loop systems with very poor robustness similar. We can thus conclude that it is a fundamental difference between using sensors for all states and reconstructing the states using an observer.

## $H_\infty$ Control



Robust control design is called  $H_\infty$  for reasons that will be explained shortly. The basic ideas are simple but the details are complicated and we will therefore just give the flavor of the results. A key idea is illustrated in Figure 12.15 where the closed loop system is represented by two blocks, the process  $P$  and the controller  $C$ . The process  $P$  has two inputs, the control signal  $u$  which can be manipulated by the controller, and the generalized disturbance  $w$ , which represents all external influences, for example command signals and disturbances. The process has two outputs, the generalized error  $z$  which is a vector of error signals representing the deviation of signals from their desired values and the measured signal  $y$  which can be used by the controller to compute  $u$ . For a linear system and a linear controller the closed loop system can be represented the linear system

$$z = H(P(s), C(s))w \quad (12.16)$$

which tells how the generalized error  $w$  depends on the generalized disturbances  $w$ . The control design problem is to find a controller  $C$  such that the gain of the transfer function  $H$  is small even when the process has uncertainties. There are many different ways to specify uncertainty and gain, giving rise to different designs. The names  $H_2$  and  $H_\infty$  control corresponds to the corresponding norms  $\|H\|_2$  and  $\|H\|_\infty$ .

To illustrate the ideas we will consider a regulation problem for the system in Figure 12.9. The reference signal is assumed to be zero and the external signals are the load disturbance  $d$  and the measurement noise  $n$ . The generalized input is  $w = (-n, d)$ . (The negative sign of  $n$  is not essential, it is chosen taken to get somewhat nicer equations.) The generalized error is chosen as  $z = (x, v)$ , where  $x$  is the process output, and  $v$  which the part of the load disturbance that is not compensated by the controller Figure 12.9. The closed loop system is thus modeled by

$$z = \begin{pmatrix} x \\ v \end{pmatrix} = H(P, C) \begin{pmatrix} -n \\ d \end{pmatrix} = \begin{pmatrix} \frac{1}{1+PC} & \frac{P}{1+PC} \\ \frac{C}{1+PC} & \frac{PC}{1+PC} \end{pmatrix} \begin{pmatrix} -n \\ d \end{pmatrix}, \quad (12.17)$$

which is the same as equation (12.16). A straight forward calculation shows that

$$\|H(P, C)\|_\infty = \sup_\omega \frac{\sqrt{(1 + |P(j\omega)|^2)(1 + |C(j\omega)|^2)}}{|1 + P(j\omega)C(j\omega)|}. \quad (12.18)$$

There are efficient numerical methods to find a controller such that  $\|H(P, T)\|_\infty < \gamma$ , if such a controller exist. The best controller can then be found by iterating on  $\gamma$ . The calculations can be made by solving *algebraic Riccati* equations for example by using the command `hinfscn` in MATLAB. The controller has the same order as the process, and the same structure as the controller based on state feedback and an observer, see Figure 7.5 and Equation (7.17).

Notice that if we minimize  $\|H(P, T)\|_\infty$  we make sure that the transfer functions  $G_{yd} = P/(1 + PC)$ , that represent transmission of load disturbances to the output, and  $G_{un} = -C/(1 + PC)$ , that represent how measurement noise is transmitted to the control signal, are small. Since the sensitivity and the complementary sensitivity functions are also elements of  $H(P, C)$  we have also guarantees that the sensitivities are also less than  $\gamma$ . The design methods thus balances performance and robustness.

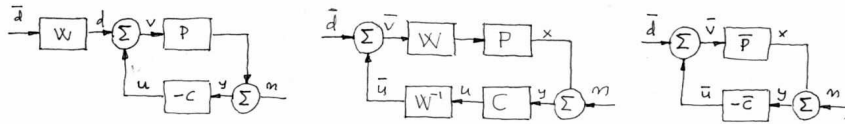


Figure 12.16: Block diagrams of a system with disturbance weighting.

### Disturbance Weighting

Minimizing the gain  $\|H(P, C)\|_\infty$  means that gains of all individual signal transmissions from disturbances to outputs are less than  $\gamma$  for all frequencies of the input signals. The assumption that the disturbances are equally important and that all frequencies are also equally important is not very realistic, recall that load disturbances typically have low frequencies and measurement noise is typically dominated by high frequencies. It is straight forward to modify the problem so that disturbances of different frequencies are given different emphasis, by introducing a weighting filter on the load disturbance as shown in Figure 12.15. For example low frequency load disturbances will be enhanced by choosing  $W_d$  as a low pass filter because the actual load disturbance is  $W_d \bar{d}$ . By using block diagram manipulation as shown in Figure 12.16 we find that the system with frequency weighting is equivalent to the system with no frequency weighting in Figure 12.16 and the signals are related through

$$z_w = \begin{pmatrix} x \\ \bar{v} \end{pmatrix} \begin{pmatrix} \frac{1}{1 + P_w C_w} & \frac{P_w}{1 + P_w C_w} \\ \frac{C_w}{1 + P + w C_w} & \frac{P_w C_w}{1 + P_w C_w} \end{pmatrix} \begin{pmatrix} -n \\ \bar{d} \end{pmatrix} = H(P_w, C_w) w_w \tag{12.19}$$

where  $P_w = P W_d$  and  $C_w = W_d^{-1} C$ . The problem of finding a controller  $C_w$  which minimizes the gain of  $H(P_w, C_w)$  is thus equivalent to the problem without disturbance weighting, having obtained  $C_w$  the controller for the original system is then  $C = W_d C_w$ . Notice that if we introduce the frequency weighting  $W_d = k/s$  we will automatically get a controller with integral action.

### Robustness

There are strong robustness results associated with the  $H_\infty$  controller. We can understand this intuitively by comparing Equations (12.1) and (12.18). We can then conclude that

$$\|H(P, C)\|_\infty = \frac{1}{d(P, -1/C)} \quad (12.20)$$

The inverse of  $\|H(P, C)\|_\infty$  is thus equal to chordal distance between  $P$  and  $1/C$ . If we find a controller  $C$  with  $\|H(P, C)\|_\infty < \gamma$  this controller will then stabilize any process  $P_*$  such that  $d(P, P_*) < \gamma$ .

### Limits of Robust Design

There is a limit to what can be achieved by robust design. In spite of the nice properties of feedback there are situations where the process variations are so large that it is not possible to find a linear controller which gives a robust system with good performance. It is then necessary to use other controllers. In some cases it is possible to measure a variable that is well correlated with the process variations. Controllers for different parameters values can then be designed and the corresponding controller can be chosen based on the measured signal. This type of controller is called *gain scheduling*. The cruise controller is a typical example where the measured signal could be gear position and velocity. Gain scheduling is the common solution for high performance aircraft where scheduling is done based on Mach number and dynamic pressure. When using gain scheduling it is important to make sure that switches between the controllers do not create undesirable transients.

If it is not possible to measure variables related to the parameters, it is possible to use *automatic tuning* and *adaptive control*. In automatic tuning process dynamics is measured by perturbing the system and a controller is then designed automatically. Automatic tuning requires that parameters remain constant, it has been widely applied for PID control, it is a reasonable guess that, in the future, many controllers will have features for automatic tuning. If parameters are changing it is possible to use adaptive methods where where process dynamics is measured on-line.

## 12.7 Further Reading

Robustness was a central issue in classical control, see [Bod45]. It was deemphasized in the euphoria of the development of design methods based

on optimization. The strong robustness of LQ control based on state feedback shown by Anderson and Moore [?] contributed to the optimism. The poor robustness of output feedback based on LQG was pointed out by Rosenbrock [RM71], Horowitz [Hor75] and Doyle [Doy78] resulted in a renewed interest in robustness. A major step forward was the development of design methods where robustness was explicitly taken into account. Seminal work by Zames [Zam81] was a major step forward. Robust control was originally developed using powerful results from the theory of complex variables which unfortunately gave controllers of very high order. A major breakthrough was given by Doyle, Glover, Khargonekar, and Francis [DGKF89] who showed that the solution could be obtained using Riccati equations and that a controller of low order could be found. This paper led to an extensive treatment of the so-called  $H_\infty$  control [Fra87, MG90, DFT92, GL95, ZDG96, SP96, Vin01]. A major advantage of the theory is that it combines much of the intuition from servomechanism theory with sound numerical algorithms based on numerical linear algebra and optimization. The results have been extended to nonlinear systems by treating the design problem as a game where the disturbances are generated by an adversary as described in [BB91]. Auto-tuning and adaptive control are treated in [ÅW95] and automatic tuning is dealt with in depth in [ÅH05].

## 12.8 Exercises

1. Show that an additive disturbance  $\delta_{add}$ , show that it can create RHP zeros, but not RHP poles, and that a feedback disturbance  $\delta_{fbk}$  can create RHP poles but not RHP zeros. Also give constructive examples.
2. Compute the distance between the systems

$$P_1(s) = \frac{k}{s+1}, \text{ and } P_2(s) = \frac{k}{s-11}.$$

for  $k = 1, 2$  and  $5$ .

3. The distance measure is closely related to closed loop systems with unit feedback. Show how the measure can be modified to applied to an arbitrary feedback.
4. Consider the Nyquist curve in Figure 12.12. Explain why part of the curve is approximately a circle. Derive a formula for the center and the radius and compare with the actual Nyquist curve.

5. Consider the transfer functions in examples 12.2 and 12.3. Compute the distance measure  $\delta(P_1, P_1)$  in both cases. Repeat the calculations when the controller is  $C = 0.1$ .
6. (Ideal Delay Compensator) Consider a process whose dynamics is a pure time delay, the transfer function is  $P(s) = e^{-s}$ . The ideal delay compensator is a controller with the transfer function  $C(s) = 1/(1 - e^{-s})$ . Show that the sensitivity functions are  $T(s) = e^{-s}$  and  $S(s) = 1 - e^{-s}$  and that the closed loop system will be unstable for arbitrary small changes in the delay.
7. Let  $P$  and  $C$  be matrices whose entries are complex numbers, show that the singular values of the matrix

$$H(P, C) = \begin{pmatrix} 1 & P \\ \frac{1}{1+PC} & \frac{P}{1+PC} \\ \frac{1}{1+PC} & \frac{P}{1+PC} \end{pmatrix}$$

are  $\sigma_1 = 0$  and  $\sigma_2 = \sup_{\omega} \frac{\sqrt{(1 + |P(j\omega)|^2)(1 + |C(j\omega)|^2)}}{|1 + P(j\omega)C(j\omega)|}$ .

8. Show that

$$\sup_{\omega} \frac{|1 + P(j\omega)C(j\omega)|}{\sqrt{(1 + |P(j\omega)|^2)(1 + |C(j\omega)|^2)}} = d(P, -1/C)$$